International Journal of Earth Sciences

The Late Neoproterozoic magmatism in the metasedimentary Ediacaran series of the Eastern Pyrenees: New ages and isotope geochemistry

--Manuscript Draft--

Manuscript Number:	
Full Title:	The Late Neoproterozoic magmatism in the metasedimentary Ediacaran series of the Eastern Pyrenees: New ages and isotope geochemistry
Article Type:	Original Paper
Keywords:	U-Pb zircon geochronology: Sr-Nd isotopes; Ediacaran magmatism; Cadomian; Pyrenees
Corresponding Author:	Josep Maria Casas Universitat de Barcelona Barcelona, SPAIN
Corresponding Author Secondary Information:	
Corresponding Author's Institution:	Universitat de Barcelona
Corresponding Author's Secondary Institution:	
First Author:	Josep Maria Casas
First Author Secondary Information:	
Order of Authors:	Josep Maria Casas
	Marina Navidad
	Pedro Castiñeiras
	Montserrat Liesa
	Carmen Aguilar
	Jordi Carreras
	Mandy Hofmann
	Andreas Gärtner
	Ulf Linnemann
Order of Authors Secondary Information:	
Abstract:	Geochronological U-Pb (LA-ICP-MS), geochemical and isotopic data from metavolcanic felsic rocks of the Canigó and Cap de Creus massifs in the Eastern Pyrenees provide evidence of an Ediacaran magmatic event lasting 30 m.y. in NE Iberia. Data also constrain the age of the Late Neoproterozoic succession in the Cap de Creus massif, where depositional ages range from 577 to 558 Ma, and in the Canigó massif, where the data (575 to 568 Ma) represent minimum ages. Geochemistry indicates that the rocks were formed in a back-arc environment and record a fragment of a long-lived subduction-related magmatic arc (620 to 520 Ma) in the active northern Gondwana margin. The homogeneity shown by all these crustal fragments along this margin suggests that the individualization of the Pyrenean basement from the Iberian Massif started later, probably during its transition from an active to a passive margin in Cambro-Ordovician times.

The Late Neoproterozoic magmatism in the metasedimentary Ediacaran series of the Eastern Pyrenees: New ages and isotope geochemistry

J.M. Casas[1,*], M. Navidad[2], P. Castiñeiras[2], M. Liesa[3], C. Aguilar[3], J. Carreras[4], M. Hofmann[5], A. Gärtner[5], U. Linnemann[5]

[1]Departament de Geodinàmica i Geofísica-Institut de recerca GEOMODELS
Universitat de Barcelona, Martí i Franquès s/n, Barcelona, 08028, Spain.
[2]Departamento de Petrología y Geoquímica, Universidad Complutense de Madrid. 28040 Madrid, Spain.
[3]Departament de Geoquímica, Petrologia i Prospecció Geològica
Universitat de Barcelona, Martí i Franquès s/n, Barcelona, 08028, Spain.
[4]Departament de Geologia, Universitat Autònoma de Barcelona, Bellaterra (Cerdanyola del Vallès), 08193, Spain.
[5]Senckenberg Naturhistorische Sammlungen Dresden, Museum für Mineralogie und Geologie, Sektion Geochronologie. Königsbrücker Landstraße 159, D-01109 Dresden, Germany

Abstract Geochronological U-Pb (LA-ICP-MS), geochemical and isotopic data from metavolcanic felsic rocks of the Canigó and Cap de Creus massifs in the Eastern Pyrenees provide evidence of an Ediacaran magmatic event lasting 30 m.y. in NE Iberia. Data also constrain the age of the Late Neoproterozoic succession in the Cap de Creus massif, where depositional ages range from 577 to 558 Ma, and in the Canigó massif, where the data (575 to 568 Ma) represent minimum ages. Geochemistry indicates that the rocks were formed in a back-arc environment and record a fragment of a long-lived subduction-related magmatic arc (620 to 520 Ma) in the active northern Gondwana margin. The homogeneity shown by all

these crustal fragments along this margin suggests that the individualization of the Pyrenean basement from the Iberian Massif started later, probably during its transition from an active to a passive margin in Cambro-Ordovician times.

Keywords U-Pb zircon geochronology, Sr-Nd isotopes, Ediacaran magmatism, Cadomian, Pyrenees

*Corresponding author. Tel.: +34 934021388; fax: +34 93401340

E-mail address: casas@ub.edu (J.M. Casas)

Introduction

Late Neoproterozoic-Early Cambrian magmatic rocks have been extensively described in the Ediacaran sequences of several areas of the European Variscan Belt (Lescuyer and Cocherie 1992; Fernández-Suárez et al. 1998; Alexandrov et al. 2001; Gutiérrez-Alonso et al. 2004; Mingram et al. 2004; Teipel at al. 2004; Alexandre 2007; Melleton et al. 2010; Rubio-Ordóñez et al. 2013) and in the Variscan basement rocks involved in the Mediterranean Alpine orogens (Cocherie et al. 2005; Micheletti et al. 2007; Castiñeiras et al. 2008; Williams et al. 2012; Fiannacca et al. 2013). These magmatic rocks, which constitute the most important evidence of the Cadomian orogeny in these areas, are associated with the later stages of the long-lived active margin that resulted from a Gondwana directed subduction of a former (Protothetys or Iapetus?) peri-Gondwanan ocean. These rocks also provide valuable information about the northern continental margin of Gondwana during its transition from active to passive in Cambro-Ordovician times (Eguiluz et al. 2000; Nebauer 2002; Murphy et al. 2004; Simancas et al. 2004; Linnemann et al. 2007; Nance et al. 2010). In most cases, the geochemical and isotopic studies of these igneous rocks enable us to assess the age of the pre-

Ordovician metasedimentary sequences and correlate them along the whole margin. Should these studies not be undertaken, the ages of these sequences would remain unresolved because of the intensity of the Variscan and/or the Alpine deformation and metamorphism, the lack of fossiliferous content and the absence of reference stratigraphic horizons (Gutiérrez-Alonso et al. 2004; Rodríguez-Alonso et al. 2004; Talavera et al. 2012). This is the case of the basement of the Pyrenees, where Ediacaran magmatic rocks are interbedded in or intrude into a thick pre-Silurian series and constitute the only age constraint for the lower segment of this sequence (Cocherie et al. 2005; Castiñeiras et al. 2008; Mezger 2010). This pre-Silurian material exhibits characteristics that hamper their correlation with the classic zones defined in the Iberian Massif, suggesting a different evolution during Ordovician times. In the Pyrenees, we can highlight the absence of a thick Early Ordovician detrital sequence, the presence of Late Ordovician magmatism and the evidence of Ordovician deformation (see discussion in Navidad et al. 2010). These characteristics pose some interesting questions about when this divergent evolution started and about the position of the Ediacaran rocks of the Pyrenees in the Gondwana margin.

In order to discuss these topics, we present new geochemical, isotopic and geochronological data from Late Neoproterozoic magmatic rocks of the Canigó and Cap de Creus massifs of the Eastern Pyrenees. These data allow us to characterize the pre-Variscan geodynamic evolution of this segment of the northern Gondwana margin and could help us to understand the paleogeography of the northern margin of Gondwana in Ediacaran times.

Geological setting

The presence of pre-Variscan igneous rocks in the pre-Silurian basement rocks of the Pyrenees have been reported by Guitard and Laffitte (1956) and Cavet (1957). These authors described metavolcanic acid rocks with a porphyritic texture, known as *gneiss granulé* (granular gneiss). These rocks are located in the lower part of a thick (up to 5000? m) unfossiliferous metasedimentary series. This series is composed of metapelites and metagreywackes and interbedded with numerous layers of marbles, quartzites and calc-silicates and is cut by orthogneiss bodies. In the Canigó massif (Fig. 1), Guitard (1970), Casas et al. (1986), Ayora and Casas (1986) and Navidad and Carreras (2002) also described greenschists and amphibolites derived from basaltic lava flows, diabasic dikes and gabbro bodies mainly located in the middle and lower part of this succession (Fig. 2). The close location of metavolcanic acid and basic rocks indicate that this bimodal magmatism may be coeval. The age of this lower series in the Canigó massif has been obtained by analyzing the U-Pb system in zircon by SHRIMP (Cocherie et al. 2005; Castiñeiras et al. 2008). However, the amount of inherited zircon hampers a straightforward interpretation of the isotopic data, resulting in two contrasting ages of 581 and 560 Ma, respectively (Fig. 2 and 3a) (Table 1). In addition, several bodies of augen orthogneisses (up to 2000 m thick) derived from Ordovician intrusives (Cocherie et al. 2005; Casas et al. 2010) are present in this lower part of the succession. In the neighboring Roc de Frausa massif (Fig. 1), metatuffs have been assigned a Late Neoproterozoic age (548±8 Ma, SHRIMP U-Pb in zircon Castiñeiras et al. 2008) for the uppermost part of the succession. The Mas Blanc orthogneiss located in the lower part of the Roc de Frausa massif has yielded a Late Neoproterozoic age (560±7 Ma, SHRIMP U-Pb in zircon, Castiñeiras et al. (2008). Nevertheless, because of its intrusive character, it cannot be used to determine the age of the lowermost part of the series since it only provides a minimum depositional age. This succession is overlain by a rhythmic alternation of sandstones, siltstones and argillites, 1500 m thick, with no metavolcanic intercalations (Fig. 2). This upper segment was recently dated using an acritarch assemblage that yielded a Late Cambrian (Furongian) to Early Ordovician age (Casas and Palacios 2012).

In contrast, the Cap de Creus massif is mainly made up of a 1000 m thick monotonous alternation of predominant greywackes, with subordinate pelites and discontinuous layers of plagio-amphibolites, banded quartzites and marbles that correspond to the lower segment of the pre-Silurian sequence. Metabasites crop out at the bottom and in the middle part of this sequence whereas metatuffs are mainly interstratified at the top (Fig. 2 and 3b) (Navidad and Carreras 1995). Metabasites proceed from gabbro-dolerite intrusions and basaltic lens-shaped bodies, and metatuffs derive from Al-rich calc-alkaline rhyolites and rhyodacites (Navidad and Carreras 1995). Metatuffs are interbedded with carbonaceous black slates and marbles. They yielded a Late Neoproterozoic age (560±10 Ma, SHRIMP U-Pb in zircon, Castiñeiras et al. 2008) (Table 1). The uppermost outcropping levels are conglomerates, siliciclastic sediments and carbonates with marked lateral changes (Losantos et al. 1997). In contrast with the Canigó massif, no large aluminous augen ortthogneiss bodies derived from Ordovician intrusives are present, and only a 200 m thick sub-aluminous subvolcanic orthogneiss body (the so-called Port gneiss, Carreras and Ramírez 1984) crops out at the bottom of the sequence. Its protolith corresponds to a small intrusion of quartz-monzonite that yielded 553±4.4 Ma (SHRIMP U-Pb in zircon Castiñeiras et al. 2008) (Table 1). Thus, the Port gneiss can be regarded as the plutonic equivalent of the metavolcanic rocks located in the upper part of the sequence.

A well-dated Upper Ordovician succession (Cavet 1957; Hartevelt 1970) lies unconformably over the former sequences (Santanach 1972a; García-Sansegundo and Alonso 1989; Den Brok 1989; Kriegsman et al. 1989; Casas and Fernández 2007) (Fig. 3a). Although it is not easy to evaluate the magnitude of this unconformity, it may be assumed that there was considerable erosion before the Upper Ordovician deposition, because Upper Ordovician rocks overlie different sections of the pre-Upper Ordovician succession in the Central and Eastern Pyrenees (Santanach 1972a; Laumonier and Guitard 1986; Cirés et al. 1994; Muñoz et al. 1994). During the Silurian, black shales were deposited, which grade upwards to alternating black limestones and shales. The Devonian is represented by a limestone sequence, whereas the Carboniferous is made up of a detrital sequence (Culm facies) composed of slates with sandstones and conglomerates that unconformably overlie the aforementioned sequence.

Variscan deformation (Late Visean to Serpukhovian) accompanied by high-temperature–low-pressure metamorphism affected all these sequences (Guitard 1970; Zwart 1979). Syn to late orogenic granitoids (Late Bashkirian-Kasimovian, Romer and Soler 1995; Maurel 2003; Aguilar et al. 2013 and references therein) intruded mainly into the upper levels of the succession. It should be noted that in the Pyrenees no tectono-metamorphic event related to the Cadomian orogeny has been described hitherto and that only a weakly developed Ordovician deformation (Mid? to Late Ordovician in age) has been reported (Casas 2010), giving rise to folds without cleavage development and to normal faults. Finally, the Alpine cycle did not lead to a considerable penetrative deformation in the Variscan basement rocks (Muñoz 1992).

Sampling rationale

As stated above, the age of the lower sequence in the Canigó massif is only constrained by radiometric data although the two U-Pb studies in zircon have yielded different ages. In order to better constrain the age of the interbedded volcanism and therefore the age of this succession, we selected three samples of acid metavolcanic rocks of the middle part of the series and three samples of metabasites of the lower part of the series on the southern slope of the massif (Fig. 2 and 3a). Using the standard separation methods, only the acid metavolcanic rocks yield zircons and thus the age of the lowermost part of the succession remains unresolved.

Samples TG-07-01, TG-7-02 and TG-07-03 correspond to feldspathic ignimbrites collected near TreguRà in an area where the metavolcanic rocks attain their maximum development (up to 500 m thick). These metavolcanic rocks are located in the same stratigraphic position as those studied by Cocherie et al. (2005) and Castiñeiras et al. (2008) (Figs. 2 and 3a). They are formed by heterometric rock fragments mostly of volcanic origin and minor bedrock fragments (limestones and greywackes) from 3-5 cm in size. The matrix is granular to mud-size with crystal fragments of feldspar and quartz resembling *gneiss granulé*. These rocks are interbedded with other sedimentary rocks, including black shales, sandstones and limestones and have been previously described as conglomerates (Cirés et al. 1994). However, it is possible to detect, at outcrop and thin section scales, ample evidence of their volcanic origin. Sample TG-07-01 corresponds to an ignimbrite of andesitic-dacitic composition. It is a heterogeneous rock formed by elongated rock fragments in a groundmass with millimetric feldspars. It is formed by plagioclase and quartz porphyroclasts in a foliated microcrystalline matrix. Plagioclase is subidiomorphic to xenomorphic, and quartz is rounded and embayed. The matrix is heterogeneous with varying mineral contents in different areas, suggesting that it was originally formed by rock fragments. However, deformation has blurred the limits of the rock fragments, hampering their distinction. In some cases, the matrix is composed of quartz, feldspar, phengitic muscovite, chlorite and calcite. Zircon and ilmenite are the main accessory minerals. Replacements of K-feldspar by albite and myrmekitic quartz are frequent. Leucoxene, and locally titanite, replace ilmenite. Leucoxene is generally associated with calcite. Two foliations can be observed, defined by secondary muscovite, chlorite and iron ore. The first foliation is folded, forming a well-developed axial plane foliation. Calcite crystallizes as plates in the matrix and in pressure shadows around plagioclase porphyroclasts. Sample TG-07-02 corresponds to an andesitic-dacitic ignimbrite alternating with ampelitic black layers. Feldspar and quartz porphyroclasts (1-2 mm in size) are embedded in a fine-grained foliated recrystallized groundmass made up of quartz, feldspar, chlorite, calcite and white mica with leucoxene and clinozoisite as accessory minerals. The groundmass exhibits shards recrystallized to sericite. Quartz porphyroclasts are locally embayed and formed by subgrains. Sample TG-07-03 is an andesitic ignimbrite similar to the samples described above. Under the microscope, it presents plagioclase and quartz porphyroclasts in a fine-grained recrystallized groundmass formed by aggregates of roughly equidimensional quartz and feldspar. Rounded and embayed quartz is usually broken and cemented by the matrix. Abundant ignimbrite textures are present in the matrix, such as glass shards and glass spherulitic textures replaced by leucoxene.

In the Cap de Creus massif, three acid metavolcanic rocks and three metabasites were sampled for U-Pb zircon analysis in order to determine the age of the bimodal magmatism and to better constrain the age of the Ediacaran sequence in this massif (Figs. 2 and 3b). Again, no zircon was detected in the metabasites.

Sample CC-08-01 corresponds to a decimeter sized metatuff located at the bottom of the sequence, whereas samples CC-08-07 and CC-08-08 are metatuffs located on top of the succession (Fig. 2). Sample CC-08-01 is a very fine-grained amphibolic leucogneiss. It corresponds to an ash tuff or lava of trachyandesitic composition. The metamorphic mineral assemblage is quartz, albite and white mica, estilpnomelane and scarce green amphibol (edenitic hornblende) with zircon, tourmaline, leucoxene and iron ore as accessory minerals. It has a porphyroclastic texture with a grano-lepidoblastic groundmass. Quartz and feldspar (mostly plagioclase) porphyroclasts range between 0,1-0,2 mm in size. They have a rounded to elongated shape with crystal faces. Polysynthetic twinning is abundant in plagioclase and some feldspars also present Carlsbad twinning. Porphyroclasts are wrapped by white mica defining the main foliation. Sample CC-08-07 corresponds to an andesitic metatuff with porphyroclastic texture and a grano-lepidoblastic matrix. Porphyroclasts are scarce and are mainly formed by plagioclase. They are between 0,2-0,3 mm in size, though some crystals attain 1 mm. The groundmass is grano-lepidoblastic and is composed of quartz, white mica, actinolite, chlorite, titanite and calcite. Plagioclase is partly replaced by clinozoisite. Muscovite defines a foliation. Ignimbritic textures are recognized as shards and flames recrystallized to sericite. Sample CC-08-08 corresponds to a metatuff of basaltic andesite composition. It has a porphyroclastic texture in a very fine-grained groundmass. The metamorphic mineral assemblage is formed by quartz, albite and chlorite with leucoxene, zircon and ilmenite as accessory minerals. Porphyroclasts (up to 2 mm in size) are composed of quartz and of plagioclase with polysynthetic twinning fragmented and welded by the matrix. The groundmass is formed by recrystallized quartz and feldspar and by newly formed metamorphic chlorite exhibiting a preferred orientation. Chlorite also crystallizes in pressure shadows around the porphyroclasts.

Results

Whole-rock geochemistry

Whole-rock analyses were carried using ICP-OES (Inductively Coupled Plasma-Optical Emission Spectrometry) for major and minor elements, and ICP-MS (Inductively Coupled Plasma-Mass Spectrometry) for trace elements at the Spectrochemical Laboratory of the Centre de Recherches en Pétrographie et Géochimie of Nancy (France). See Online Resource 1 for analytical details. Results are given in Table 2.

Acid porphyroclastic tuffs and ashes have been classified using conventional diagrams for presumably modified rocks based on trace elements, such as Zr/Ti vs. Nb/Y (Winchester and Floyd 1977) and Th vs. Co (Hastie et al. 2007) (Fig. 4). Most of the samples cluster along the line between the andesite and dacite-rhyodacite fields (Fig. 4a) or inside the dacite-rhyolite (Fig. 4b), depending on the diagram used. In the Hastie et al. (2007) diagram, the samples also plot in the high K calc-alkaline domain.

A trace element diagram normalized to the ORG (Harris et al. 1986) is presented in Fig. 5a. All the samples show similar profiles characterized by an enrichment of the mobile elements (K, Rb, Ba, Th, excepting sample CC-08-08), a negative Ta-Nb anomaly and a positive Ce and Sm anomalies. They also show a relative enrichment of the transition elements with respect to the immobile elements. These patterns are characteristic of the calc-alkaline and shoshonite series in volcanic arcs (Pearce et al. 1984).

In a REE chondrite normalized (Taylor and McLennan 1985) diagram (Fig. 5b), the patterns are very similar. All the samples are enriched in light REE (LREE) with respect to the heavy REE (HREE), and show a moderate fractionation (with LREE/HREE ratios between 6.5 and 11) and a slight negative Eu anomaly (Eu/Eu* between 0.52 and 0.65). These patterns are typical of calc-alkaline rocks with plagioclase fractionation and without the participation of garnet. In the Cap de Creus samples, it is important to note that CC-08-01 and CC-08-07 (amphibole-bearing tuffs) are more depleted in total REE (□REE=165 and 119, respectively) than CC-08-08, a non amphibolic ignimbrite with □REE= 246.

As regards the geodynamic setting (Fig. 6), most of the samples plot between the volcanic arc and the within-plate fields in a Hf-Rb/30-Tax3 diagram (Harris et al. 1986).

Isotopic geochemistry

Sr-Nd isotope analyses were performed at the Geochronology and Isotope Geochemistry Centre of the Complutense University (Madrid, Spain) using ID-TIMS in a sector 54 VG-Micromass Multicollector Spectrometer. Details of the analytical procedures are given in the Online Resource 1. The Sr-Nd isotope results are shown in Table 3.

Most of the samples show a relatively homogeneous $^{87}Sr/^{86}Sr$ isotopic content with ratios between 0.704474 and 0.709730. The lowest value in sample TG-07-01 probably represents a disturbance of the Rb-Sr isotopic system, whereas the maximum value in sample CC-08-08 could be related to crustal contamination. In contrast, the $^{143}Nd/^{144}Nd$ ratios are more uniform, varying between 0.511679 and 0.511884. For the epsilon notation, all samples were normalized to an age of 560 Ma. The □Nd values were moderately enriched for most of the samples (below -4.0), with the exception of sample CC-08-01, which had a less enriched value of -0.6 (Fig. 7a, Table 3). In the □Sr-□Nd diagram (Fig. 7b), it should be noted that the variability observed in the Cap de Creus between sample CC-08-01 and sample CC-08-08, in the Sr and the Nd systems is compatible with a fractionation and a variable crustal contamination of juvenile mantle-derived melts (Navidad and Carreras 1995). Alternatively, the Canigó samples (excepting sample TG-07-01) plot in a narrow area of the young continental crust field.

Zircon geochronology

The volcaniclastic nature of the analyzed samples gives rise to a large amount of inherited and/or detrital zircon, ruling out the possibility of precise dating of these rocks in the Canigó massif (Cocherie et al. 2005; Castiñeiras et al. 2008). To overcome this problem, we use the LA-ICP-MS technique (Laser Ablation, Inductively Coupled Plasma, Mass Spectrometry) to analyze the U, Th, and Pb isotopes in zircon since we can obtain more data much faster than with the SHRIMP. The analyses were carried out at the Museum für Mineralogie und Geologie (Senckenberg Naturhistorische Sammlungen Dresden), using a Thermo-Scientific Element 2 XR sector field ICP-MS coupled to a New Wave UP-193 Excimer laser system. Details of the analytical procedure and the results of the zircon analyses are shown in Online Resource 1 and 2.

Under cathodoluminescence (CL), most zircons from the Canigó samples exhibit oscillatory zoning, with scarce xenocrystic cores or metamorphic rims. Some zircon grains with homogeneous textures can be found (Fig. 8). We carried out a total of 184 analyses in as many zircon grains from the three Canigó samples selected. We disregarded 22 analyses with discordance higher than 10%. In spite of our efforts to avoid inheritance during the hand picking of the zircon grains (see analytical procedure in SD-1), the remaining 162 analyses are dispersed between 546 and 2,640 Ma. Taking into account previous works (Cocherie et al. 2005; Castiñeiras et al. 2008), we selected the analyses younger than 590 Ma to calculate the crystallization ages using the statistical methods available in Isoplot (Ludwig 2001), whereas older data were considered inheritance.

In sample TG-07-01, eleven analyses vary between 555 and 588 Ma, yielding a concordia age (sensu Ludwig 1998) of 570±5 Ma (Fig. 9a), with a mean square of weighted deviation (MSWD) of 0.43. In sample TG-07-02, nine analyses vary between 546 and 587 Ma, yielding a concordia age of 568±6 Ma, with an MSWD of 0.0056 (Fig. 9b). Twenty analyses from sample TG-07-03 vary between 564 and 588 Ma, yielding a concordia age of 575±4, with an MSDW of 0.15 (Fig. 9c).

We performed 380 analyses in zircon grains from the three Cap de Creus samples selected. We rejected 101 analyses with discordance higher than 10%. The inherited component in these samples is also significant, and the resulting ages vary between 543 and 2,554 Ma. As in the previous sample, we selected the analyses younger than 590 Ma to extract the crystallization ages, whereas older data were regarded as inheritance. In accordance with their volcano-sedimentary origin, zircons from the Cap de Creus samples display an assortment of textures under CL (Fig. 8). These textures include abundant core-rim features with variable luminescence, where cores represent xenocrysts and are surrounded by oscillatory rims of magmatic origin. Other textures comprise some homogeneous and scarce sector zoning.

In sample CC-08-01, twelve analyses vary between 568 and 590 Ma, yielding a concordia age (sensu Ludwig 1998) of 577±3 Ma (Fig. 10a), with an MSWD of 0.23. In sample CC-08-07, twenty-two analyses vary between 543 and 590 Ma, yielding a concordia age of 571±5 Ma (Fig. 10b). However, the high mean square of weighted deviation (MSWD=10) suggests that more than one age population is included in this concordant dataset. For this reason, we use the Sambridge and Compston (1994) statistical approach to extract these age populations. Thus, two classes can be established, namely an older age of 580 Ma and a younger age of 561 Ma (Fig. 10c). To decide between these two possible ages, we go back to the cathodoluminescence images, where we can observe the disparity of CL textures in the oldest spots, whereas the areas that yielded the youngest ages show similar CL characteristics. Thus, we obtain the crystallization age of the rock pooling together the fourteen youngest analyses (Fig. 10b), which is 563±5 Ma (MSWD=4.2). Finally, twenty-seven analyses from sample CC-08-08 vary between 539 and 579 Ma, yielding a concordia age of 558±3, with an MSDW of 2.8 (Fig. 10d).

Discussion

Petrogenesis, tectonic setting and age

The homogeneous patterns shown in the ORG-normalized trace element and in the chondrite-normalized REE diagrams suggest that all the samples were formed in the same tectonic setting. Furthermore, the high potassium content, the relative enrichment in large ion lithophile elements associated with high field strength elements and the Nb-Ta negative anomaly indicate that this setting was an active continental margin.

However, the whole-rock and isotope geochemistry of the samples reveal a subtle difference in their petrogenesis. On the one hand, the enrichment in εNd in the Canigó samples (TG-07-01, 02 and 03) lends support to our interpretation and highlights the influence of old material. The TDM ages (~1.5 Ga, Fig. 7a) do not correspond to the ages found hitherto in inherited zircons (Cocherie et al. 2005; Castiñeiras et al. 2008). It should be noted that none of these studies focused on inheritance with result that sampling bias could arise. The U-Pb ages obtained from zircon are equivalent within error in all the samples and indicate that the magmatism in the Canigó massif took place around 570 Ma. On the other hand, the Cap de Creus samples (CC-08-01, 07 and 08) show some differences among them, not only in their chemistry and age, but also in their petrography. The presence of amphibole in two samples, the low REE contents and the less enriched □Nd values in samples CC-08-01 and CC-08-07 suggest an influence of a juvenile source in the origin of these rocks. Furthermore, the trend observed in Fig. 7b is interpreted in this work as the result of a combination of fractionation and crustal contamination between a juvenile mantle source and an enriched crust. The ages obtained in these rocks are less homogeneous than in the Canigó, varying between 558 and 577 Ma. In addition, the enrichment in Nd is higher in the youngest samples, i.e. the influence of the juvenile source (probably the mantle) decreased with time. This evolution is compatible both with the closure of an oceanic domain and with the thickening of a previous thinned crust, probably in a back-arc setting. The absence of ophiolites in the Ediacaran section of the Pyrenees and the abundance of coeval mafic lavas interbedded in the Ediacaran series of the Cap de Creus massif (Navidad and Carreras 1995) favor the latter possibility.

With the available data, it is not clear whether the juvenile influence is restricted to the Cap de Creus massif or whether it also affected the magmatism in the Canigó massif. If the former option were correct, both massifs would represent two slightly different scenarios in the active continental margin, a small back-arc basin (Cap de Creus) and a zone with more continental influence (Canigó). Further studies on the influence of a juvenile source are necessary in the Canigó massif to either confirm or reject this interpretation.

An additional contribution of this work is the refinement in the age of the Ediacaran magmatism. The data presented here as well as previous published data provide evidence of an Ediacaran magmatic event lasting 30 m.y. in NE Iberia. In this area, volcanic activity seems to be continuous from 577 to 548 Ma, whereas granite production took place between 560 and 553 Ma. Earlier studies (Cocherie et al. 2005; Castiñeiras et al. 2008) report ages obtained by SHRIMP using a limited amount of data (less than 25 analyses in each work).

However, the abundance of inherited zircons in these volcaniclastic rocks hampers the interpretation of the preferred age in these studies. In fact, there is a variation of ~20 m.y. from one work to another. Furthermore, even if the best smoothest zircon grains are selected to avoid detrital or inherited components in areas where a protracted active margin exists, it is not easy to distinguish between zircons formed during the last magmatic event and short-traveled zircons from closer and slightly older domains. In this case, the number of analyses should be increased to obtain a more reliable and representative set of the youngest population, which is interpreted as the age of magmatism. Given its higher velocity when compared with the SHRIMP technique, the LA-ICP-MS is the ideal choice to accomplish the task.

Data also constrain the depositional age of the Late Neoproterozoic succession in the Cap de Creus and Canigó massifs. In the Cap de Creus massif, depositional ages range from 577 to 558 Ma, whereas the age obtained for the metavolcanic rocks of the Canigó massif (575 to 568 Ma) should be regarded as the minimum because of a thick series cropping out below these rocks in this massif. It should be noted, that these ages were only obtained in felsic rocks and that the age of the protoliths of the metabasites is still unknown. However, we can consider a similar Late Neoproterozoic age for the metabasaltic lava flows interbedded in the lower part of the succession although the protolith age of the plutonic metabasites remains to be resolved and a younger pre-Variscan (Ordovician?) age cannot be ruled out. Further geochemical and geochronological studies are warranted to elucidate this problem.

Comparison with neighboring areas

This magmatism may be part of a longer cycle, as revealed by the distribution of magmatic ages obtained in neighboring areas. In the French Massif Central, a magmatic event ranging from Late Neoproterozoic (617±17 Ma, Alexandre 2007 and 574±28 Ma, Melleton et al. 2010) to Early Cambrian (525±12 Ma, Alexandrov et al. 2001; 526±14 Ma, Alexandre 2007 and 529±4 Ma, Melleton et al. 2010) has been described in the metasedimentary successions of the different structural units. On the Montagne Noire, south of the French Massif Central, metavolcanic rocks provided an age of 545±15 Ma for the ”schistes X” in the uppermost part of the Late Neoproterozoic succession (Lescuyer and Cocherie 1992). These data reinforce the aforementioned correlation between the lowermost series of the Eastern Pyrenees and the Montagne Noire based on lithostratigraphic criteria (Cavet 1957) or on the strong similarities of the metallogenic assemblages (Ayora and Casas 1986). In the Iberian Massif, a magmatic cycle of a similar age has been described. In the Narcea Antiform, between the Cantabrian and Western Asturian-Leonese zones, Late Neoproterozoic ages ranging from 605±10 Ma to 557±3 Ma for plutonic and volcanic rocks intruded or interlayered in the Neoproterozoic siliciclastic series have been obtained by Fernandez-Suárez et al. (1998), Gutiérrez-Alonso et al. (2004) and Rubio Ordóñez et al. (2013). In the Ossa Morena zone, Bandrés et al. (2004) describe diorite and granite bodies intruding at 577.6±0.6 Ma and 573±14 Ma. All these authors agree that this Late Neoproterozoic-Early Cambrian magmatism is related to a convergent margin setting, which is a subduction-related magmatic arc.

A similar situation has been reported in other Mediterranean Variscan realms involved in the Alpine orogens. In the basement rocks of the Calabria-Peloritani Mountains (southern Italy and NE Sicily), Michelletti et al. (2007), Williams et al. (2012) and Fiannacca et al. (2013) describe an important Late Neoproterozoic-Early Cambrian magmatism ranging from 565±5 to 526±10 Ma. From the age of zircon cores Williams et al. (2012) and Fiannacca et al. (2013) propose a proximity between the depositional age of the Neoproterozoic sequences and the age of the plutonic rocks, indicating a short time span between sedimentation and generation of granitic rocks. In the Menderes massif (western Taurides), Zlatkin et al. (2013) describe a similar situation: bimodal Late Neoproterozoic magmatic rocks intruded from 550.6±1.1 to 544 Ma in a sequence that exhibits a very close sedimentation age from ~570 Ma to 550 Ma. Finally, in the Late Neoproterozoic basement rocks of the western Pontides, Yilmaz Şahin et al (2013) reported granites with similar ages from 546±3.9 to 534±4.7 Ma.

Given the available geochronological and geochemical data and the results presented in this paper, it may be argued that the studied rocks record a fragment of a long-lived subduction-related magmatic arc (620 to 520 Ma) in the active northern Gondwana margin. This margin can be recognized in the Variscan belt of western and central Europe. Furthermore, the fragments of Ediacaran rocks recognized in the Mediterranean orogens suggest that the margin can be extended eastwards through the Turkish massif as far as the Iranian and Caucasus Mountains (see discussion in Yilmaz Şahin et al. (2013).

The homogeneity shown by all these crustal fragments along the Gondwana margin indicates that the individualization of the Pyrenean basement with respect to the Iberian Massif would have started later, probably during its transition from an active to a passive margin in Cambro-Ordovician times.

Conclusions

The geochemistry of felsic metavolcanic rocks in the upper part of the Ediacaran series from the Canigó and Cap de Creus massifs indicates a convergent setting for their origin. In the Cap de Creus massif isotope geochemistry suggests a juvenile influence in their petrogenesis whereas in the Canigó massif the crustal component is more important. The U-Pb ages obtained reveal that this volcanism took place around 570 Ma in the Canigó massif but in Cap de Creus the volcanic event spanned from 558 through 577 Ma.

The rocks under study display characteristics similar to those of other Cadomian remnants found in the Variscan and Alpine basement, which taken together represent a convergent margin located in northern Gondwana from 620 through 520 Ma. The partition between the Pyrenean domain and the Iberian Massif probably occurred in Cambro-

Ordovician times, when the tectonic setting underwent a transition from an active to a passive margin.

Acknowledgements This work was funded by projects CGL2010-21298 and Consolider-Ingenio 2010, under CSD2006-00041 "Topoiberia".

References

Aguilar C, Liesa M, Castiñeiras P, Navidad M (2013) Late Variscan metamorphic and magmatic evolution in the eastern Pyrenees revealed by U–Pb age zircon dating. Journal of the Geological Society London. doi:org/10.1144/jgs2012-086.

Alexandre P (2007) U–Pb zircon SIMS ages from the French Massif Central and implication for the pre-Variscan tectonic evolution in Western Europe. Comptes Rendus Geoscience 339: 613-621.

Alexandrov P, Floc'h J-P, Cuney M, Cheilletz A (2001) Datation U–Pb à la microsonde ionique des zircons de l'unité supérieure de gneiss dans le Sud Limousin, Massif central. Comptes Rendus de l'Académie des Sciences 332: 625-632.

Ayora C, Casas JM (1986) Strabound As-Au mineralization in pre-Caradocian rocks form the Vall de Ribes, Eastern Pyrenees, Spain. Mineralium Deposita 21**:** 278-287.

Bandrés A, Eguíluz L, Pin C, Paquette J. L, Ordóñez B, Le Fèvre B, Ortega LA, Gil Ibarguchi J I (2004) The northern Ossa-Morena Cadomian batholith (Iberian Massif): magmatic arc origin and early evolution. International Journal of Earth Sciences 93: 860–885.

Carreras J, Ramírez J (1984) The geological significance of the Port de la Selva Gneisses (Eastern Pyrenees, Spain). IGCP Newsletter 6: 27-31.

Carreras J, Druguet E (2013) Illustrated Field Guide to the Geology of Cap de Creus. Servei de Publicacions de la Universitat Autònoma de Barcelona.

Casas JM (2010) Ordovician deformations in the Pyrenees: new insights into the significance of pre-Variscan ('sardic') tectonics. Geological Magazine 147: 674–689.

Casas JM, Martí J, Ayora C (1986) Importance du volcanisme dans la composition lithostratigraphique du Paléozoïque inférieur des Pyrénées catalanes. Comptes Rendus de l'Académie des Sciences 302: 1193-1198.

Casas JM, Fernandez O (2007) On the Upper Ordovician unconformity in the Pyrenees: New evidence from the La Cerdanya area. Geologica Acta 5: 193-198.

Casas JM, Castiñeiras P, Navidad M, Liesa M, Carreras J (2010) New insights into the Late Ordovician magmatism in the Eastern Pyrenees: U–Pb SHRIMP zircon data from the Canigó massif. Gondwana Research 17: 317–324.

Casas J.M, Palacios T (2012) First age data obtained by Acritarchs in the pre-Upper Ordovician sequences of the Pyrenees: on the Late Cambrian-Early Ordocivian age of the Jujols Series. Comptes Rendus Geosciences 344: 50-56.

Castiñeiras P, Navidad M, Liesa M, Carreras J, Casas J.M (2008) U-Pb zircon ages (SHRIMP) for Cadomian and Lower Ordovician magmatism in the Eastern Pyrenees: new insights in the pre-Variscan evolution of the northern Gondwana margin. Tectonophysics 46:, 228-239.

Cavet P (1957) Le Paléozoïque de la zone axiale des Pyrénées orientales françaises entre le Roussillon et l'Andorre. Bulletin Service Carte Géologique France 55**:** 303-518.

Cirés J, Casas JM, Santanach P, Muñoz J.A, Fleta J, Serrat D (1994(Mapa geológico de España (1:50.000): Molló (nº 218). ITGE Madrid, España.

Cocherie A, Baudin Th, Autran A, Guerrot C, Fanning C.M, Laumonier B (2005) U-Pb zircon (ID-TIMS and SHRIMP) evidence for the early Ordovician intrusion of metagranites in the late Proterozoic Canaveilles Group of the Pyrenees and the Montagne Noire (France). Bulletin de la Société Géologique de France 176: 269-282.

DePaolo DJ (1981) Neodymiun isotopes in the Colorado Front range and crust-mantle evolution in the Proterozoic. Nature 291: 193-196.

Den Brok SWJ (1989) Evidence for pre-Variscan deformation in the Lys Caillaouas area, Central Pyrenees, France. Geologie en Mijnbouw 68: 377-380.

Eguiluz L, Gil Ibarguchi JI, Ábalos B, Apraiz A (2000) Superposed Hercynian and Cadomian orogenic cycles in the Ossa-Morena zone and related areas of the Iberian Massif. Geological Society of America Bulletin 112: 1398-1413. doi: 10.1130/0016-7606(2000)112<1398:SHACOC>2.0.CO;2

Fernández-Suárez J, Gutiérrez Alonso G, Jenner G, Simon EJ (1998) Geochronology and geochemistry of the Pola de Allande granitoids (northern Spain): their bearing on the Cadomian-Avalonian evolution of northwest Iberia. Canadian Journal of Earth Sciences 35: 1439-1453.

Fiannacca P, Williams IS, Cirrincione R, Pezzino A (2013) The augen gneisses of the Peloritani Mountains (NE Sicily): Granitoid magma production during rapid evolution of the northern Gondwana margin at the end of the Precambrian. Gondwana Research 23: 782-796. doi: 10.1016/j.gr.2012.05.019

García-Sansegundo J, Alonso JL, (1989) Stratigraphy and structure of the southeastern Garona Dome. Geodinamica Acta 3: 127-134.

Guitard G, 1970. Le métamorphisme hercynien mésozonal et les gneiss oeillés du massif du Canigou (Pyrénées orientales). Mémoires du B.R.G.M. 63.

Guitard G, Laffitte F, (1956) Sur l'importance et la nature des manifestations volcaniques dans le Paléozoïque des Pyrénées Orientales. Comptes Rendus de l'Académie des Sciences 242: 2749-2752.

Gutiérrez-Alonso G, Fernández-Suárez J, Jeffries TE (2004) Age and setting of the Upper Neoproterozoic Narcea Antiform volcanic rocks. Geogaceta 25: 79-82.

Harris NBW, Pearce JA, Tindle AG (1986) Geochemical characteristics of collision-zone magmatism. In: Coward, M.P. and Ries, A.C. (Eds.), Collision tectonics. Geological Society Special Publication 19: 67-81.

Hastie AR, Kerr AC, Pearce JA, Mitchell SF (2007) Classification of altered volcanic island arc rocks using immobile trace elements: Development of the Th–Co discrimination diagram. Journal of Petrology 48: 2341-2357. doi:10.1093/petrology/egm062

Hartevelt JJA (1970) Geology of the upper Segre and Valira valleys, central Pyrenees, Andorra/Spain. Leidse Geologische Mededelingen 45: 167-236.

Kriegsman LM, Aerden DGAM, Bakker RJ, den Brok SWJ, Schutjens PMTM (1989) Variscan tectonometamorphic evolution of the eastern Lys- Caillaouas massif, Central Pyrenees-evidence for late orogenic extension prior to peak metamorphism. Geologie en Mijnbouw 68: 323-333.

Laumonier B, Guitard G (1986) Le Paléozoïque inférieur de la moitié orientale de la Zone Axiale des Pyrénées. Essai de synthèse. Comptes Rendus de l'Académie Sciences Paris 302: 473-478

Lescuyer JL, Cocherie A (1992) Datation sur monozircons des métadacites de Sériès: arguments pour un âge protérozoïque terminal des schistes X de la Montagne Noire (Massif central français). Comptes Rendus de l'Académie des Sciences 314: 1071-1077.

Linnemann U, Gerdes A, Drost K, Buschmann B (2007) The continuum between Cadomian orogenesis and opening of the Rheic Ocean: Constraints from LA-ICP-MS U-Pb zircon dating and analysis of plate-tectonic setting (Saxo-Thuringian zone, northeastern Bohemian Massif, Germany). In: Linnemann U, Nance RD, Kraft P, Zulauf G (eds.), The evolution of the Rheic Ocean: From Avalonian-Cadomian active margin to Alleghenian-Variscan collision: Geological Society of America Special Paper 423: 61-96. doi: 10.1130/2007.2423(03)

Losantos M, Palau J, Carreras J, Druguet E, Santanach P, Cirés J (1997) Mapa geològic de Catalunya, Escala 1:25.000 Fulls: Roses 259-1-1, Cap de Creus, 259-2-1, Far de Roses 259-1-2. ICC Barcelona, España.

Ludwig KR (1998) On the treatment of concordant uranium-lead ages. Geochimica et Cosmochimica Acta 62; 665-676.

Ludwig KR (2001). Users Manual for Isoplot/Ex rev. 2.49. Berkeley Geochronology Center Special Publication No. 1a, 1-56.

Maurel O, Respaut JP, Monié P, Arnaud N, Brunel M (2004) U–Pb emplacement and 40Ar/39Ar cooling ages of the eastern Mont-Louis granite massif (eastern Pyrenees, France). Comptes Rendus Geosciences 336: 1091–1098.

Melleton J, Cocherie A, Faure M, Rossi P (2010) Precambrian protoliths and Early Paleozoic magmatism in the French Massif Central: U-Pb data and the North Gondwana connection in the west European Variscan belt. Gondwana Research 17: 13-25. doi: 10.1016/j.gr.2009.05.007

Mezger JE (2010) Cadomian, Ordovician and Variscan igneous events preserved in gneiss domes of the Central Pyrenean Axial Zone. 13. Symposium "Tektonik, Struktur- und Kristallingeologie" (TSK 13), Frankfurt, April 6-12, 2010. TSK 13 Conference abstracts and field guides, 40.

Micheletti F, Barbey P, Fornelli A, Piccarreta G, Deloule E (2007). Latest Precambrian to Early Cambrian U-Pb zircon ages of augen gneisses from Calabria (Italy), with inference to the Alboran microplate in the evolution of the peri-Gondwana terranes. International Journal of Earth Sciences 96: 843-860. doi: 10.1007/s00531-006-0136-0

Mingram B, Kröner A, Hegner E, Krentz O (2004) Zircon ages, geochemistry, and Nd isotopic systematics of pre-Variscan orthogneisses from the Erzgebirge, Saxony (Germany), and geodynamic interpretation. International Journal of Earth Sciences 93: 706–727.

Muñoz J.A (1992) Evolution of a continental colision belt:ECORS-Pyrenees crustal balanced cross-section. In: Mc Clay KR (ed.), Thrust Tectonics, London: Chapman & Hall. 235-246.

Muñoz JA, Vergés J, Martínez-Rius A, Fleta J, Cirés J, Casas JM, Sàbat F (1994) Mapa geológico de España (1:50.000): Ripoll (nº 256). ITGE Madrid, España.

Murphy JB, Pisarevsky·SA, Nance RD, Keppie JD (2004) Neoproterozoic-Early Paleozoic evolution of peri-Gondwanan terranes: implications for Laurentia-Gondwana connections. International Journal of Earth Sciences 93: 659-682. doi: 10.1007/s00531-004-0412-9

Nance RD, Gutiérrez-Alonso G, Keppie JD, Linneman, U, Murphy JB, Quesada C, Strahan RA. Woodcock NH (2010). Evolution of the Rheic Ocean. Gondwana Research 17: 194-222.

Navidad M, Carreras J (1995) Pre-Hercynian magmatism in the eastern Pyrenees (Cap de Creus and Albera Massifs) and its geodynamical setting. Geologie en Mijnbouw: 74, 65-77.

Navidad M, Carreras J (2002) El volcanismo de la base del Paleozoico Inferior del Canigó (Pirineos Orientales). Evidencias geoquímicas de la apertura de una cuenca continental. Geogaceta 32: 91-94.

Navidad M, Castiñeiras P, Casas JM, Liesa M, Fernández Suárez J, Barnolas A, Carreras J, Gil-Peña I (2010) Geochemical characterization and isotopic age of Caradocian magmatism in the northeastern Iberian Peninsula: Insights into the Late Ordovician evolution of the northern Gondwana margin. Gondwana Research 17: 325–337.

Neubauer F (2002) Evolution of late Neoproterozoic to early Paleozoic tectonic elements in Central and Southeast European Alpine mountain belts: review and synthesis. Tectonophysics 352: 87-103. doi: 10.1016/S0040-1951(02)00190-7

Pearce JA, Harris NGW, Tindle AG (1984) Trace element discrimination diagrams for the tectonic interpretation of granitic rocks. Journal of Petrology 25: 956-983. doi:10.1093/petrology/25.4.956

Rodríguez-Alonso M D, Peinado M. López-Plaza M, Franco P, Carnicero A, Gonzalo JC (2004) Neoproterozoic–Cambrian synsedimentary magmatism in the Central Iberian Zone (Spain): geology, petrology and geodynamic significance. International Journal of Earth Sciences 93: 897-920.

Romer RL, Soler A (1995) U-Pb age and lead isotopic characterization of Au-bearing skarn related to the Andorra granite. Mineralium Deposita 30: 374-383.

Rubio-Ordónez A, Gutiérrez-Alonso G, Valverde-Vaquero P, Cuesta A, Gallastegui G, Gerdes A, Cárdenes V (2013) Arc-related Ediacaran magmatism along the northern margin of Gondwana: Geochronology and isotopic geochemistry from northern Iberia. Gondwana Research, in press. doi: 10.1016/j.gr.2013.09.016

Sambridge MS, Compston W (1994) Mixture modeling of multi-component data sets with application to ion-probe zircon ages. Earth and Planetary Science Letters 128: 373-390.

Santanach PF (1972a) Sobre una discordancia en el Paleozoico inferior de los Pirineos orientales. Acta Geológica Hispánica 7**:** 129-132.

Santanach PF (1972b) Estudio tectónico del Paleozoico inferior del Pirineo entre la Cerdaña y el río Ter. Acta Geológica Hispánica 7**:** 44-49.

Simancas JF, Expósito I, Azor A, Martínez Poyatos D, González Lodeiro F (2004) From the Cadomian orogenesis to the Early Paleozoic Variscan rifting in Southwest Iberia. Journal of Iberian Geology 30: 53-71.

Talavera C, Montero P, Martínez Poyatos D, Williams IS (2012) Ediacaran to Lower Ordovician age for rocks ascribed to the Schist–Graywacke Complex (Iberian Massif, Spain): Evidence from detrital zircon SHRIMP U–Pb geochronology. Gondwana Research 22: 928–942.

Taylor SR, McLennan SM (1985) The continental crust: its composition and evolution. Blackwell, Oxford.

Teipel U, Eichhorn R, Loth G, Rohrmüller J, Höll R, Kennedy A (2004) U-Pb SHRIMP and Nd isotopic data from the western Bohemian Massif (Bayerischer Wald, Germany): Implications for Upper Vendian and Lower Ordovician magmatism. International Journal of Earth Sciences 93: 782-801.

Williams IS, Fiannacca P, Cirrincione R, Pezzino A (2012) Peri-Gondwanan origin and early geodynamic history of NE Sicily: A zircon tale from the basement of the Peloritani Mountains. Gondwana Research 22: 855-865. doi: 10.1016/j.gr.2011.12.007

Winchester JA, Floyd PA (1977) Geochemical discrimination of different magma series and their differentiation products using immobile elements. Chemical Geology 20: 325-343.

Yilmaz Şahin S, Aysal N, Güngör Y, Peytcheva I, Neubauer F (2013) Geochemistry and U–Pb zircon geochronology of metagranites in Istranca (Strandja) Zone, NW Pontides, Turkey: Implications for the geodynamic evolution of Cadomian orogeny. Gondwana Research: in press. doi: 10.106/j.gr.2013.07.011.

Zlatkin O, Avigad D, Gerdes A (2013) Evolution and provenance of Neoproterozoic basement and Lower Paleozoic siliciclastic cover of the Menderes Massif (western Taurides): Coupled U–Pb–Hf zircon isotope geochemistry. Gondwana Research 23: 682–700

Zwart HJ (1979) The geology of the Central Pyrenees. Leidse Geologische Mededelingen 50, 1-74

TABLES

Table 1. Geochronological data of samples under study and those of (1) Cocherie et al. (2005) and (2) Castiñeiras et al. (2008).

Table 2. Whole-rock geochemistry of the samples from the Canigó and Cap de Creus massifs.

Table 3. Sr-Nd isotopic data for samples.

FIGURE CAPTIONS

Figure 1. Simplified geological map of the Eastern Pyrenees with the location of the areas under study.

Figure 2. Synthetic stratigraphic columns of the pre-Upper Ordovician rocks of the Canigó and Cap de Creus massifs with the location of the samples and previous geochronological data: (1) Cocherie et al. (2005), (2) Castiñeiras et al. (2008). Data from Guitard (1970), Santanach (1972b), Ayora and Casas (1986) and Losantos et al. (1997).

Figure. 3. Schematic geological maps with the location of the samples and previous geochronological data: (a) Southern flank of the Canigó massif (GRA-1, Cocherie et al. 2005; NU-3, Castiñeiras et al. 2008); (b) Cap de Creus massif (CC-05-02 and CC-05-07, Castiñeiras et al. 2008). Data from Guitard (1970), Ayora and Casas (1986), Cirés et al. (1994), Muñoz et al. (1994) and Carreras and Druguet (2013).

Figure 4. (a) Classification diagram Zr/TiO_2 versus Nb/Y (Winchester and Floyd 1977); (b) classification and character of the magma series in the Th-Co diagram (Hastie et al. 2007).

Figure 5. (a) Multi-element diagram normalized to ORG values after Harris et al. (1986) and (b) chondrite-normalized REE diagram for the rocks (normalization values after Taylor and McLennan 1985)

Figure 6. Tectonic setting discrimination diagram after Harris et al. (1986).

Figure 7. (a) eNd versus age diagram and (b) □Nd versus □Sr diagram for the analyzed samples. Depleted mantle evolution calculated according to DePaolo (1981).

Figure 8. Cathodoluminescence images for selected zircons from the analyzed samples.

Figure 9. Wetherill concordia diagrams for the Canigó samples (a) TG-07-01, (b) TG-07-02 and (c) TG-07-03. Error ellipses are plotted at 2□.

Figure 10. U-Pb results for the Cap de Creus samples; (a) (b) and (d) Wetherill concordia diagrams for samples CC-08-01, CC-08-07 and CC-08-08, (c) probability density plot showing the results of the Sambridge and Compston (1994) algorithm for sample CC-08-07 (see text for explanation). Error ellipses are plotted at 2□.

ONLINE RESOURCES

Online Resource 1. Details of the analytical procedure.

Online Resource 2. Results of the zircon analyses.

Online Resource 1 Casas et al
Click here to download Electronic Supplementary Material: Online Resource 1.doc

Online Resource 2 Casas et al
Click here to download Electronic Supplementary Material: Online Resource 2.xls

Figure 1

Click here to download high resolution image

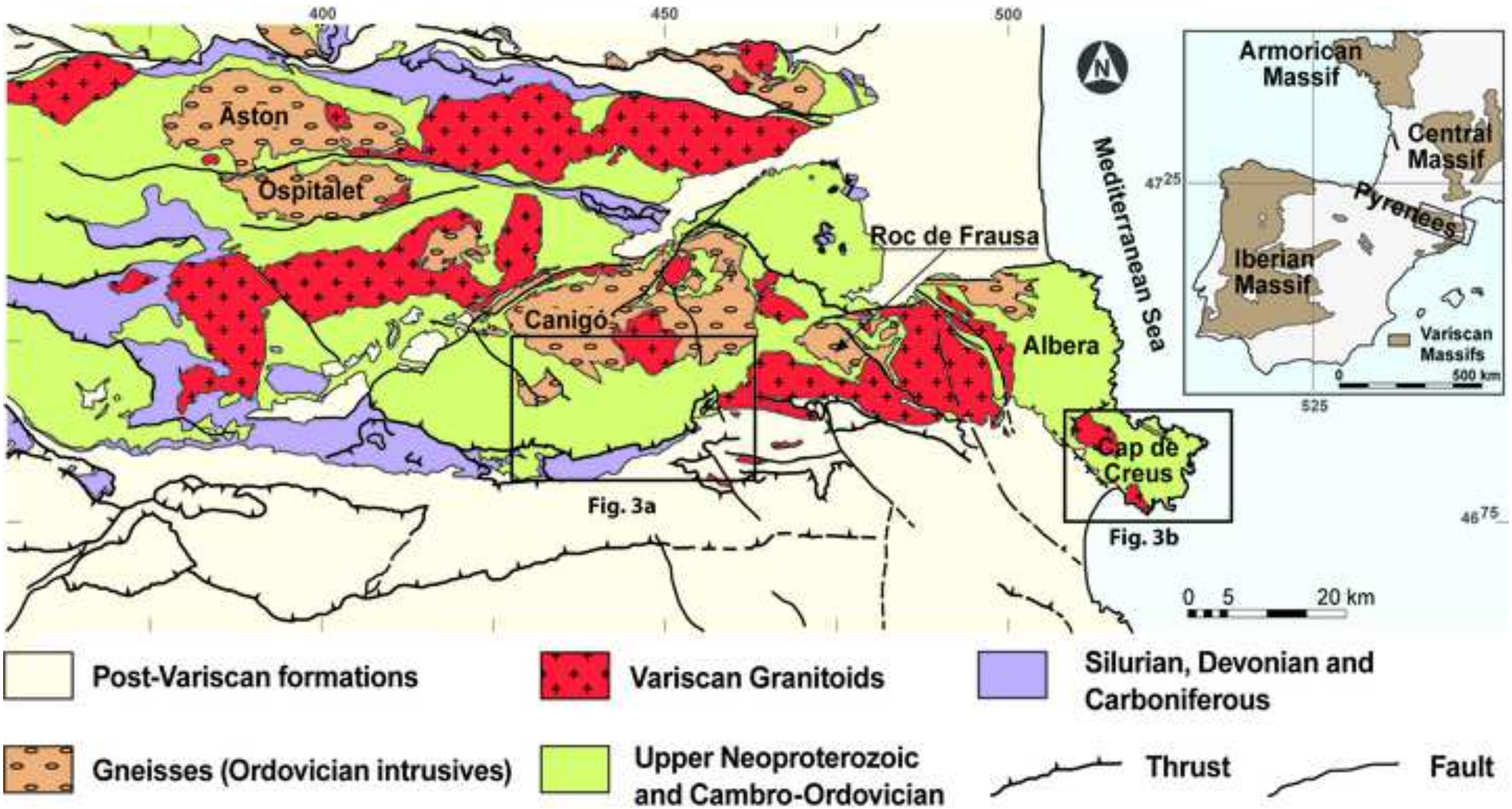

Figure 2

Click here to download high resolution image

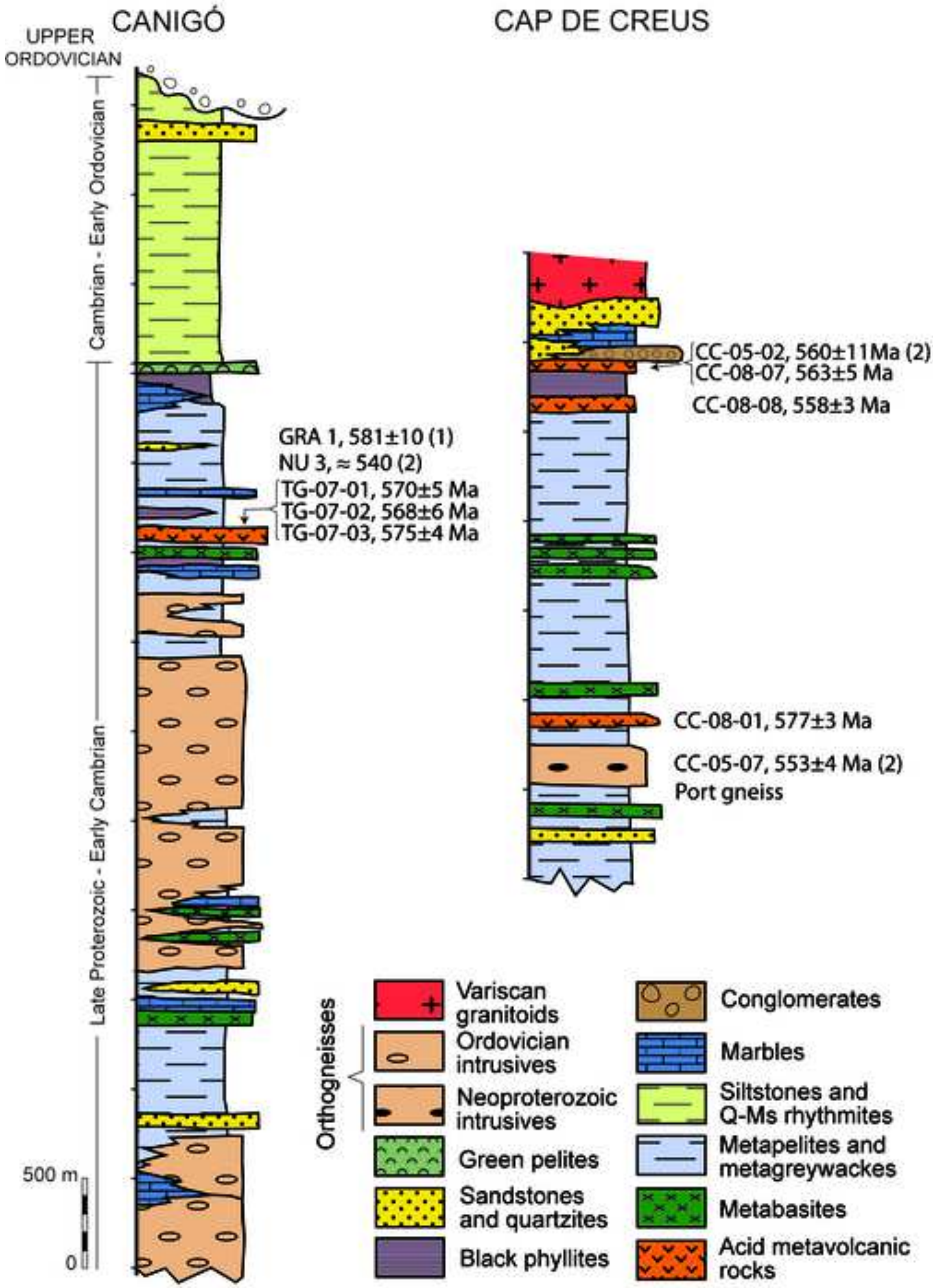

Figure 3
Click here to download high resolution image

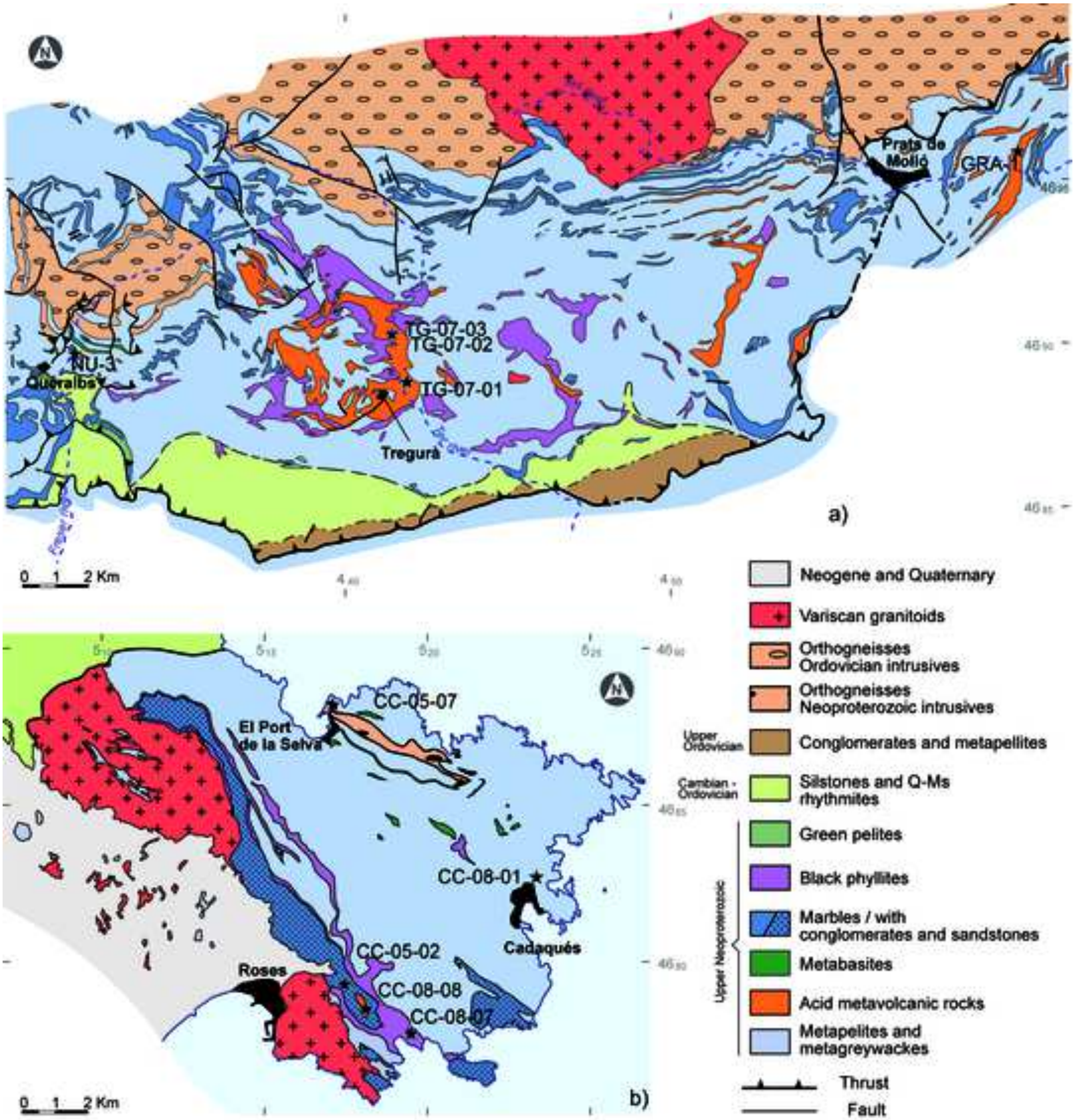

Figure 4
Click here to download high resolution image

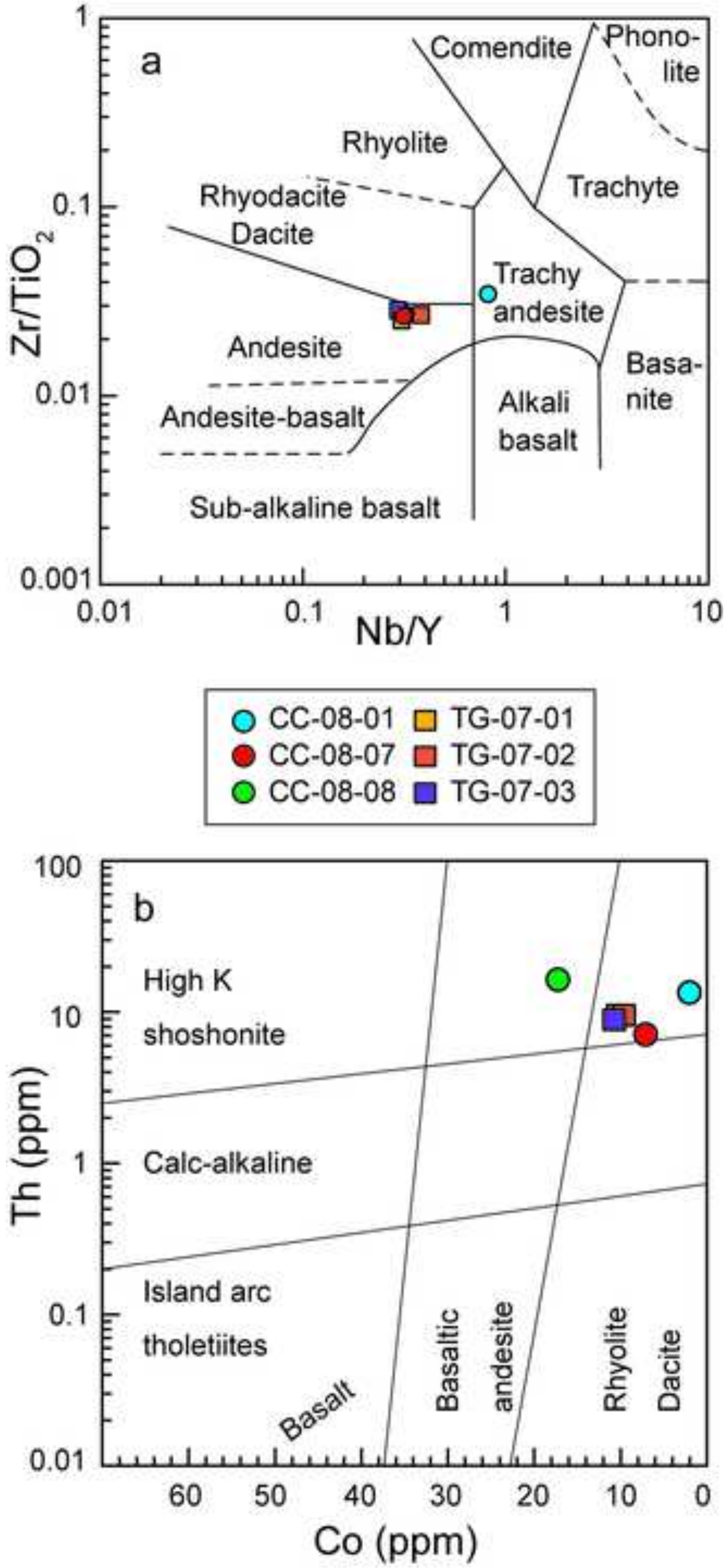

Figure 5

Click here to download high resolution image

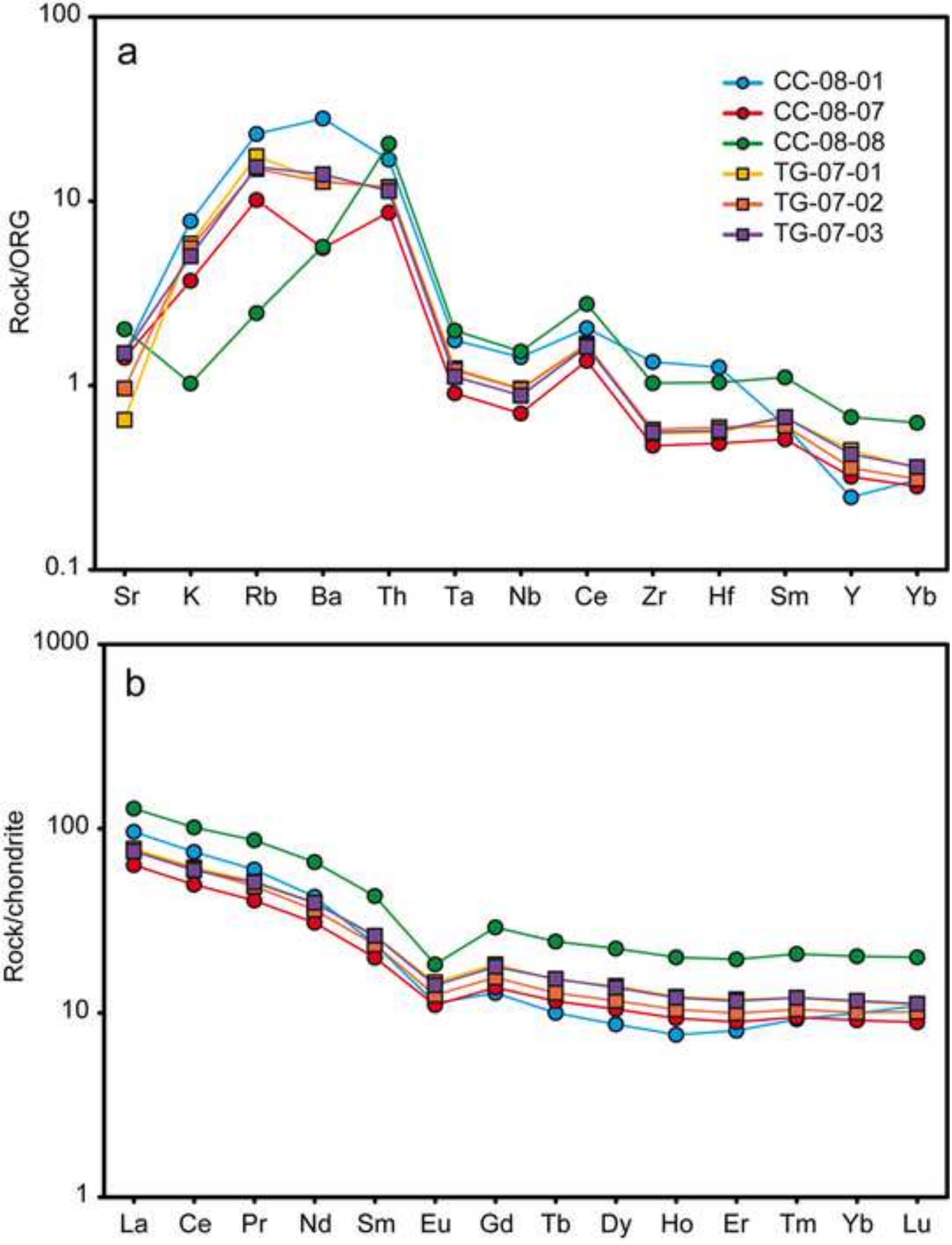

Figure 6

Click here to download high resolution image

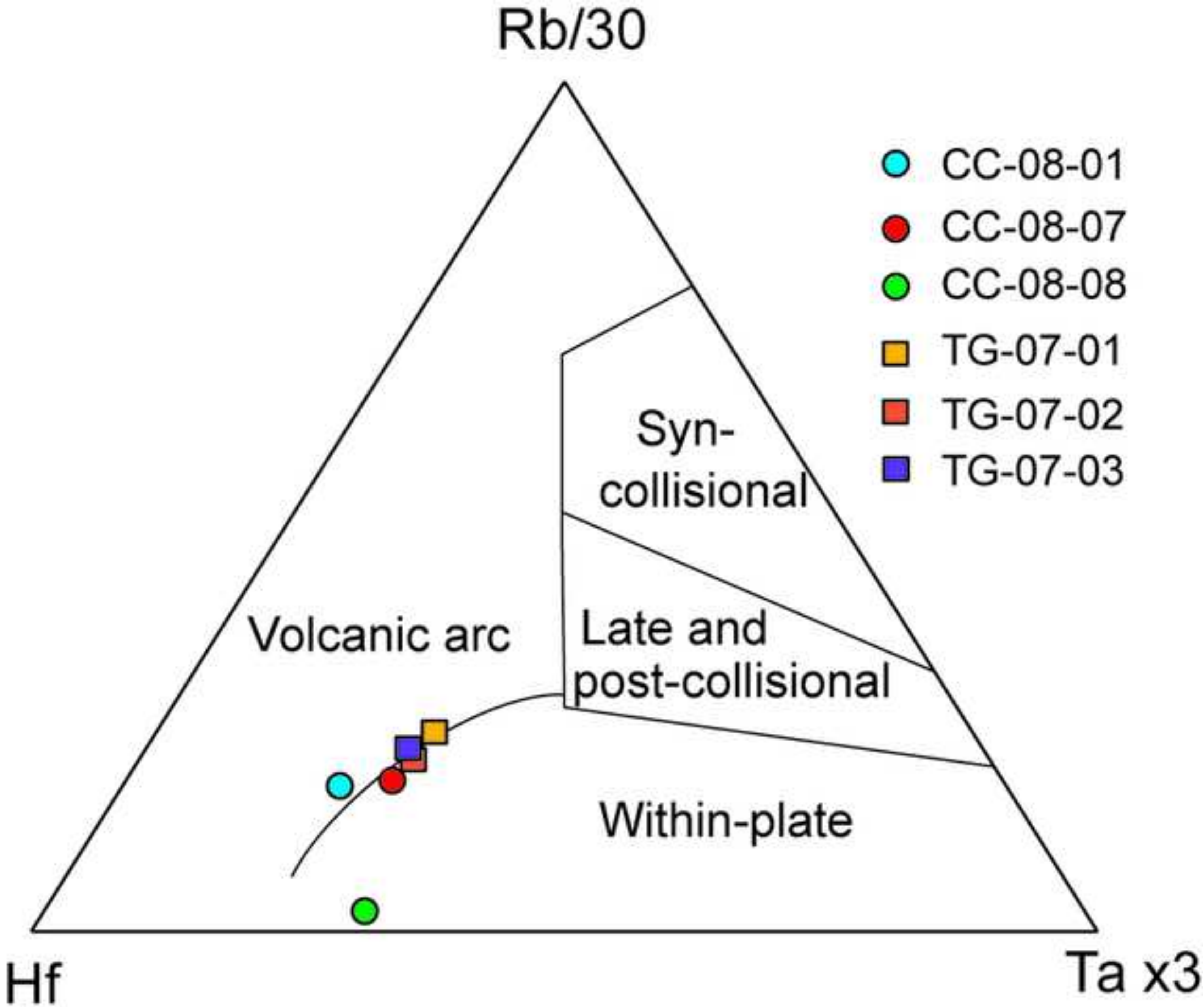

Figure 7

Click here to download high resolution image

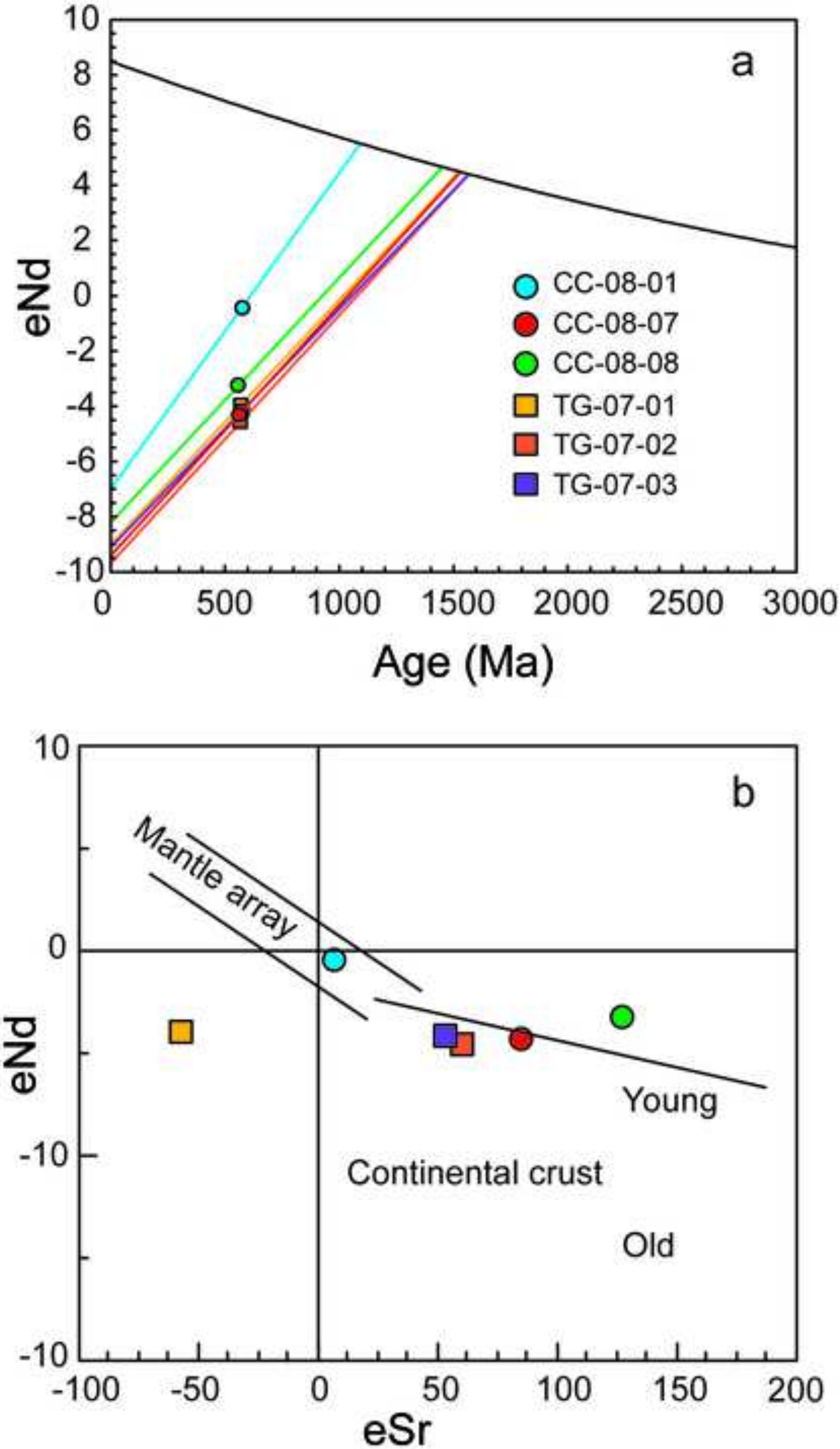

Figure 8
Click here to download high resolution image

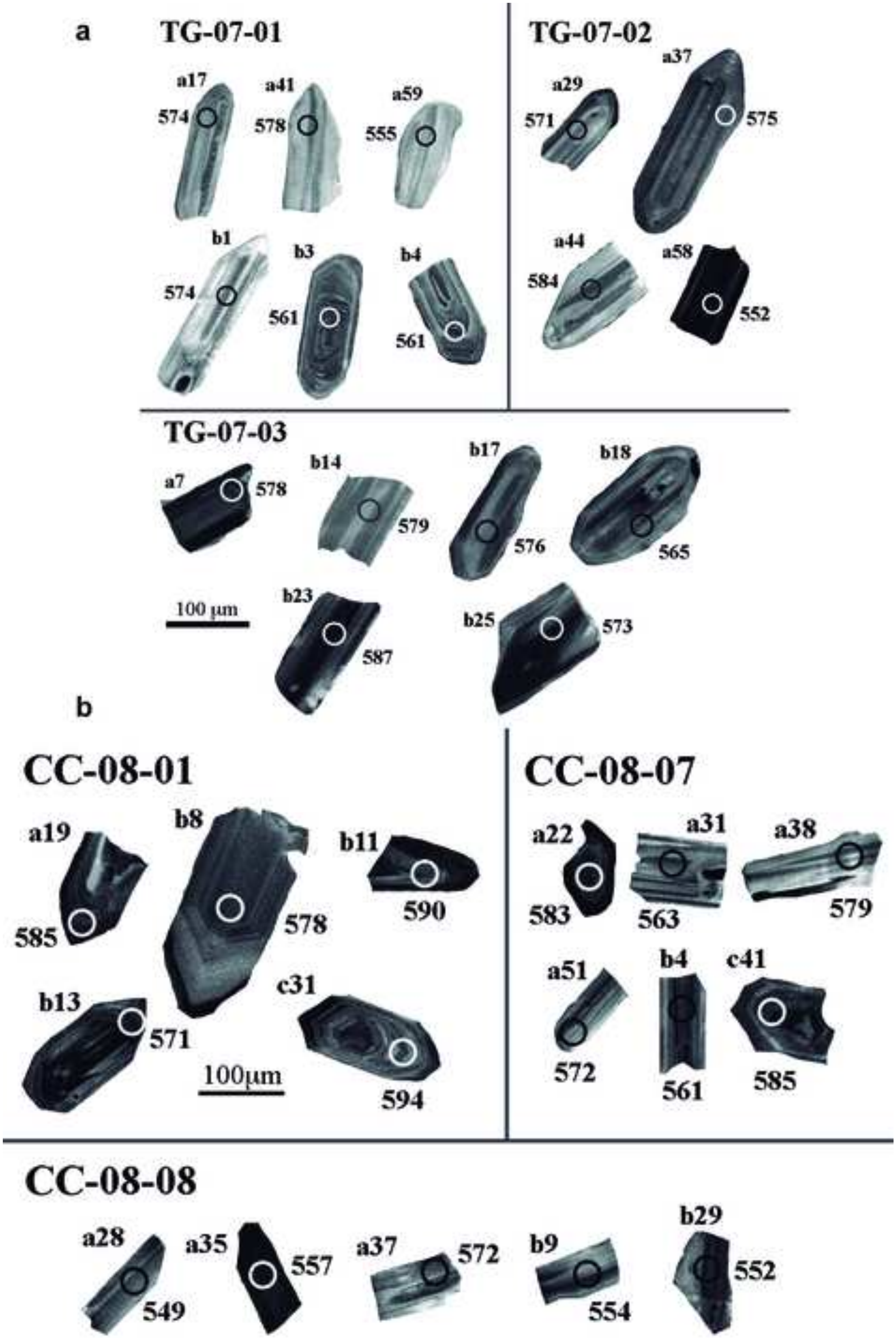

Figure 9

Click here to download high resolution image

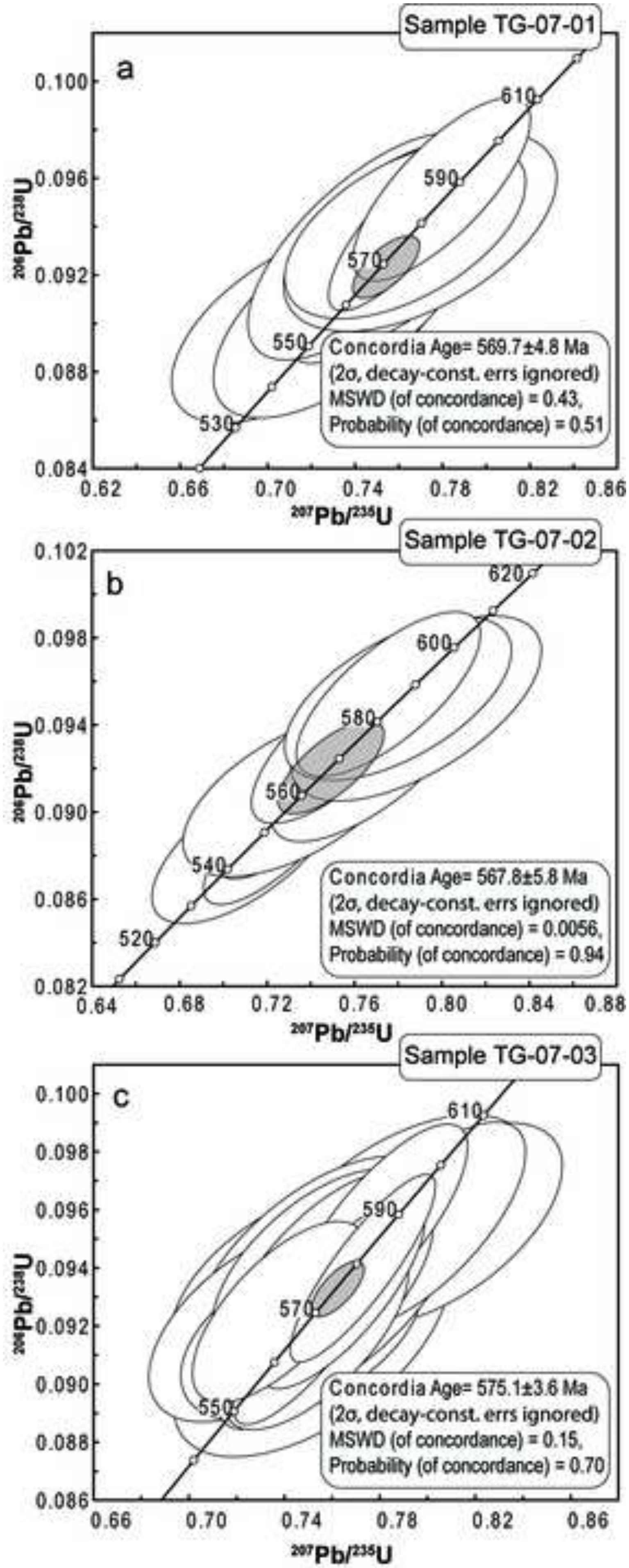

Figure 10
Click here to download high resolution image

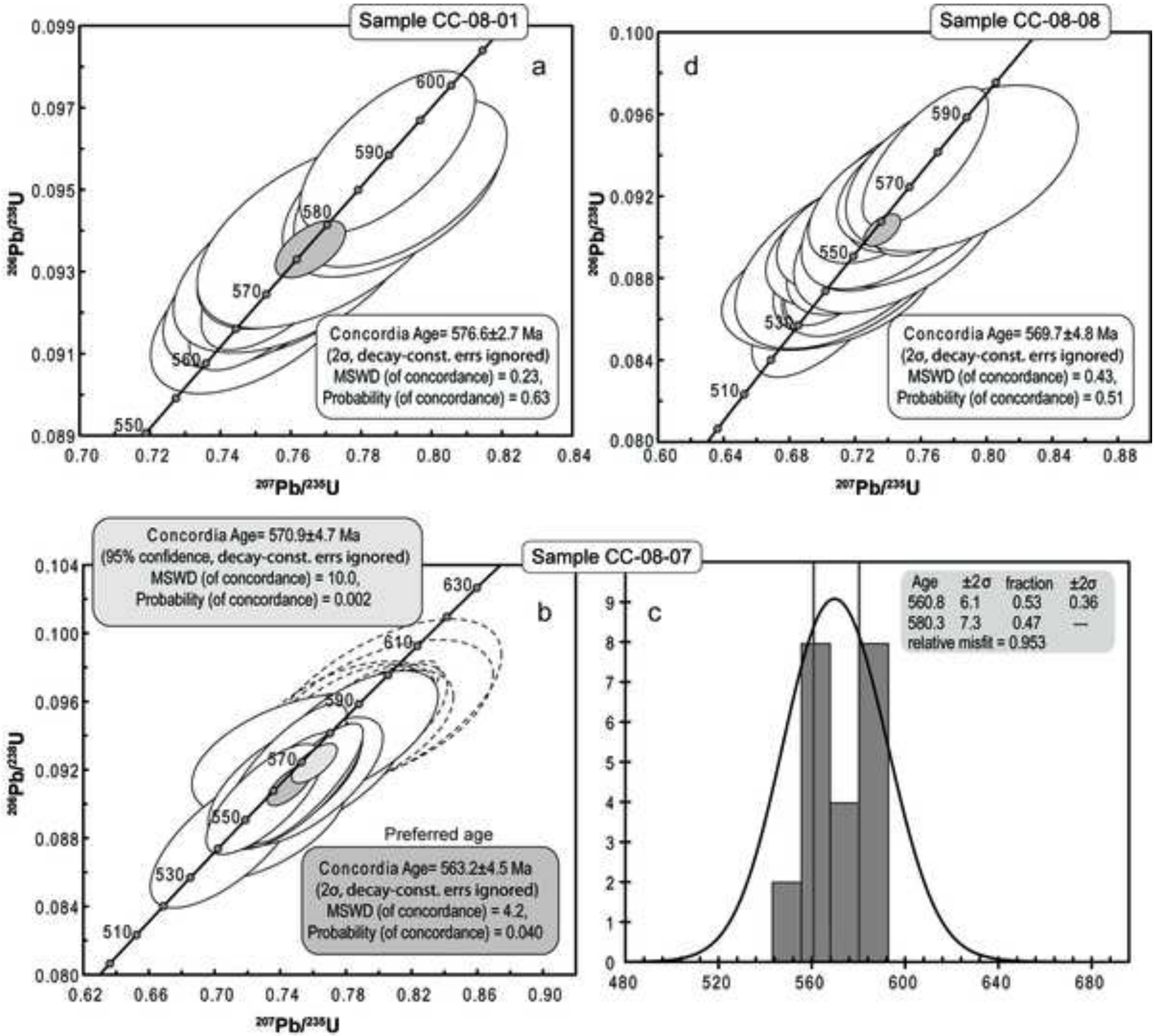

Table 1

Sample	Reference	Rock type	Age	Sampling site	X	Y
GRA I	(1)	Acid metatuff	581±10 (U-Pb SHRIMP)	Canigó massif. "Sitges" lapillis, D15 road left bank of Tec river, St. Eloi oratory.	615440	1711444
NU 3	(2)	Acid metatuff	≈ 540 (U-Pb SHRIMP)	Canigó massif. Queralbs-La Farga.	431759	4689782
RF 3	(2)	Acid metatuff	548±8 (U-Pb SHRIMP)	Roc de Frausa massif. Les Illes. Mas Quintassos.	481970	4696770
RF 4	(2)	Mas Blanc gneiss	560±7 (U-Pb SHRIMP)	Roc de Frausa massif. Mas Blanc.	482058	4696535
CC 2	(2)	Acid metatuff	560±7 (U-Pb SHRIMP)	Cap de Creus massif. Roses. Coll d'Alzeda.	517736	4679447
CC 7	(2)	Port gneiss	553±4 (U-Pb SHRIMP)	Cap de Creus massif. Port de la Selva quarry.	517582	4687795
TG-07-01	This work	Ignimbrite	570±5 (LA-ICP-MS)	Canigó massif. Tregurà. GIV5284 road, left bank of Ter river.	442098	4688717
TG-07-02	This work	Ignimbrite	568±5 (LA-ICP-MS)	Canigó massif. Tregurà. GIV5284 road, left bank of Ter river.	441882	4689874
TG-07-03	This work	Ignimbrite	575±4 (LA-ICP-MS)	Canigó massif. Tregurà. GIV5284 road, right bank of Ter river.	441683	4690200
CC-08-01	This work	Acid metatuff	577±3 (LA-ICP-MS)	Cap de Creus massif. Cadaqués. S'Alqueria Petita.	523965	4682985
CC-08-07	This work	Ignimbrite	563±5 (LA-ICP-MS)	Cap de Creus massif. Cala Montjoi, Torre Morisca.	519401	4678026
CC-08-08	This work	Acid metatuff	558±3 (LA-ICP-MS)	Cap de Creus massif. Roses-Cadaqués road. Mas de la Torre.	518226	4677333

Table 1

Table 2

	CC-08-01	CC-08-07	CC-08-08	TG-07-01	TG-07-02	TG-07-03
SiO_2	69.25	58.98	55.79	66.86	68.61	55.57
TiO_2	1.33	0.61	1.30	0.75	0.73	0.67
Al_2O_3	14.28	9.74	19.00	12.84	12.18	11.71
$Fe_2O_{3(T)}$	3.71	4.31	7.64	5.03	4.52	4.34
MnO	0.03	0.15	0.10	0.12	0.09	0.13
MgO	1.08	3.72	3.21	2.38	1.98	1.85
CaO	1.07	11.30	1.33	1.94	2.40	10.35
Na_2O	2.13	2.14	7.54	2.58	2.59	2.48
K_2O	3.12	1.48	0.41	2.35	2.23	2.01
P_2O_5	0.17	0.17	0.37	0.25	0.20	0.25
LOI	3.22	7.46	2.66	3.56	3.44	9.68
Total	99.38	100.05	99.34	98.64	98.97	99.05
Ba	1405	278	283	643	637	697
Be	1.8	< LD	< LD	1.8	1.6	< LD
Co	2.0	7.7	17	10	10	11
Cr	145	58	83	75	71	61
Cu	24	10	69	26	17	20
Ga	19	12	12	17	15	15
Hf	11	4.4	9.3	5.0	5.3	5.1
Nb	14	7.0	15	10	10	8.8
Ni	11	22	33	29	27	26
Rb	93	41	10	70	60	61
Sr	148	141	201	65	96	149
Ta	1.2	0.6	1.4	0.9	0.8	0.8
Th	13	6.9	16	10	10	9.1
U	3.8	1.9	4.1	2.4	2.2	2.5
V	137	57	113	77	75	71
Y	17	22	47	31	25	30
Zn	28	57	69	71	34	59
Zr	457	160	350	186	195	189
La	35	23	47	29	28	28
Ce	71	48	97	59	58	57
Pr	8.2	5.6	11.8	7.1	6.6	7.0
Nd	30	22	47	28	26	28
Sm	5.4	4.6	10	6.0	5.4	6.0
Eu	0.98	0.96	1.59	1.27	1.09	1.23
Gd	3.9	4.2	8.9	5.6	4.8	5.4
Tb	0.58	0.67	1.41	0.88	0.74	0.89
Dy	3.3	4.0	8.5	5.3	4.4	5.2
Ho	0.65	0.80	1.70	1.04	0.89	1.03
Er	2.0	2.2	4.9	2.9	2.5	2.9
Tm	0.33	0.34	0.74	0.43	0.37	0.43
Yb	2.5	2.3	5.0	2.8	2.5	2.9
Lu	0.42	0.34	0.76	0.42	0.39	0.43

Oxides expressed as %wt, minor and rare earth elements as ppm
$Fe_2O_{3(T)}$ expressed as total iron
LOI: Lost on ignition
<LD: below detection limit

Table 3

Table 2. Sr - Nd of Cadomian acid rocks

Samples	Sm/Nd	Rb/Sr	$(^{147}Sm/^{144}Nd)$	$(^{87}Sr/^{86}Sr)_P$	$(^{87}Sr/^{86}Sr)_{560}$	$(^{143}Nd/^{144}Nd)_P$	$(^{143}Nd/^{144}Nd)_{560}$	eNd_{560}	eSr_{560}	TDM (Ga)
TG-07-01	0.21	1.08	0.1284	3.121498	0.699797	0.512181	0.511709	-4.0	-57	1.52
TG-07-02	0.21	0.62	0.1275	1.806548	0.708024	0.512146	0.511679	-4.6	59	1.56
TG-07-03	0.22	0.41	0.1301	1.185574	0.707653	0.512175	0.511698	-4.3	54	1.55
CC-08-01	0.18	0.63	0.1083	1.812453	0.704474	0.512281	0.511884	-0.6	9	1.12
CC-08-07	0.21	0.29	0.1266	0.834941	0.709730	0.512159	0.511695	-4.3	84	1.52
CC-08-08	0.21	0.05	0.1284	0.141754	0.712765	0.512223	0.511752	-3.2	127	1.45

Table 2. Sr - Nd of Cadomian acid rocks

Age (Ma)
570
568
575
577
571
558